HHS Public Access

Author manuscript

*Arterioscler Thromb Vasc Biol*. Author manuscript; available in PMC 2019 June 01.

Published in final edited form as:

*Arterioscler Thromb Vasc Biol*. 2018 June ; 38(6): 1333–1345. doi:10.1161/ATVBAHA.118.310951.

# CaMKII ($Ca^{2+}$/calmodulin-dependent kinase II) in mitochondria of smooth muscle cells controls mitochondrial mobility, migration and neointima formation

**Emily K. Nguyen, B.S.**[1,2], **Olha M. Koval, Ph.D.**[1], **Paige Noble**[1], **Kim Broadhurst, B.S.**[1], **Chantal Allamargot, B.S.**[3], **Meng Wu, Ph.D.**[4,5,6], **Stefan Strack, Ph.D.**[7], **William H. Thiel, Ph.D.**[1,8], and **Isabella M. Grumbach, M.D., Ph.D**[1,8,9]

[1]Department of Internal Medicine, Carver College of Medicine, University of Iowa

[2]Interdisciplinary Program in Molecular and Cellular Biology, University of Iowa

[3]Central Microscopy Research Facility, Carver College of Medicine, University of Iowa

[4]Division of Medicinal and Natural Products Chemistry, Department of Pharmaceutical Sciences and Experimental Therapeutics, College of Pharmacy, University of Iowa

[5]High Throughput Screening Facility, University of Iowa

[6]Department of Biochemistry, Carver College of Medicine, University of Iowa, Iowa City, IA 52242

[7]Department of Pharmacology, Carver College of Medicine, University of Iowa, Iowa City, IA 52242

[8]François Abboud Cardiovascular Research Center, University of Iowa, Iowa City, IA 52242

[9]Iowa City Veterans Affairs Healthcare System, Iowa City, IA 52242

## Abstract

**Objective—**To define the mechanisms by which mitochondria control VSMC migration and impact neointimal hyperplasia.

**Approach and Results—**The multifunctional $Ca^{2+}$/calmodulin-dependent kinase II (CaMKII) in the mitochondrial matrix of VSMC drove a feed-forward circuit with the mitochondrial $Ca^{2+}$ uniporter (MCU) to promote matrix $Ca^{2+}$ influx. MCU was necessary for the activation of mitochondrial CaMKII (mtCaMKII), whereas mtCaMKII phosphorylated MCU at the regulatory site S92 that promotes $Ca^{2+}$ entry. mtCaMKII was necessary and sufficient for PDGF-induced mitochondrial $Ca^{2+}$ uptake. This effect was dependent on MCU. mtCaMKII and MCU inhibition abrogated VSMC migration and mitochondrial translocation to the leading edge. Overexpression of WT MCU, but not MCU S92A mutant in $MCU^{-/-}$ VSMC rescued migration and mitochondrial mobility. Inhibition of microtubule, but not of actin assembly blocked mitochondrial mobility. The

**Corresponding author:** Isabella M. Grumbach, MD, PhD, Department of Internal Medicine, Division of Cardiovascular Medicine, Carver College of Medicine, University of Iowa, 169 Newton Road, 4336 PBDB, Iowa City, IA 52242, USA, Phone: 319-384-4610, Isabella-grumbach@uiowa.edu.

**Disclosures:** One author is a named inventor on awarded patents related to targeting CaMKII inhibitors to mitochondria (OMK). All other authors declare no conflict of interest exists

outer mitochondrial membrane GTPase Miro-1 promotes mitochondrial mobility via microtubule transport, but arrests it in subcellular domains of high $Ca^{2+}$ concentrations. In Miro-$1^{-/-}$ VSMC, mitochondrial mobility and VSMC migration were abolished, overexpression of mtCaMKII or a CaMKII inhibitory peptide in mitochondria (mtCaMKIIN) had no effect. Consistently, inhibition of mtCaMKII increased and prolonged cytosolic $Ca^{2+}$ transients. mtCaMKII inhibition diminished phosphorylation of focal adhesion kinase and myosin light chain, leading to reduced focal adhesion turnover and cytoskeletal remodeling. In a transgenic model of selective mitochondrial CaMKII inhibition in VSMC, neointimal hyperplasia was significantly reduced after vascular injury.

**Conclusions—**These findings identify mitochondrial CaMKII as a key regulator of mitochondrial $Ca^{2+}$ uptake via MCU, thereby controlling mitochondrial translocation and VSMC migration following vascular injury.

### Keywords

Mitochondria; CaMKII; $Ca^{2+}$; smooth muscle cell; migration; neointima

## INTRODUCTION

Atherosclerotic vascular disease is the leading cause of mortality in the industrialized world, and commonly treated by percutaneous balloon angioplasty and stent placement. However, even with contemporary drug-eluting stents, restenosis via neointimal hyperplasia occurs after 10–30% of percutaneous arterial interventions[1]. Neointimal hyperplasia develops from excessive vascular smooth muscle cell (VSMC) migration and proliferation from the medial layer to the arterial lumen, narrowing the luminal diameter leading to decreased blood flow and recurrence of anginal symptoms[2]. Thus, neointimal hyperplasia remains a significant clinical problem in patients with vascular disease.

Previous studies have supported that mitochondrial physiology impacts on VSMC phenotypes and vascular disease such as neointimal hyperplasia[3,4], atherosclerosis,[5] and hypertension[6]. These studies primarily interrogated well-established concepts in VSMC phenotypes in vascular disease, such as mitochondrial reactive oxygen species (ROS) production and mitochondrial fission and fusion. For example, neointimal hyperplasia was blocked by delivery of mitochondrial manganese superoxide dismutase to VSMC[3]. Since mitochondria undergo dynamic fission and fusion during the cell cycle, inhibition of mitochondrial fission as anticipated decreased neointimal hyperplasia and VSMC proliferation[4]. While these studies implicate that mitochondria affect vascular function and disease, a detailed mechanistic understanding of how intra mitochondrial events alter VSMC phenotypes remains elusive.

Very recent evidence in cancer and epithelial cells has suggested that mitochondrial translocation to the leading edge is necessary to support cell mobility and invasiveness[7–10]. At the leading edge, mitochondria localize to the vicinity of focal adhesions[11] and support local energy production[7], necessary for focal adhesion turnover and cytoskeletal remodeling. Along with providing energy for VSMC, mitochondria act as major $Ca^{2+}$ buffering organelles[12,13]. Mitochondrial $Ca^{2+}$ influx is primarily controlled by mitochondrial $Ca^{2+}$

uniporter (MCU), which resides in the inner mitochondrial membrane. MCU activity is modulated by multiple regulators, including MICU and potentially multifunctional $Ca^{2+}$/calmodulin-dependent kinase II (CaMKII)[14,15]. In cancer cells, MCU inhibition perturbs cell migration[16]. For example, studies in breast cancer[17] and cervical cancer[18] cells demonstrated that migratory capacity directly correlates with the expression of MCU or its regulator MICU. The mechanisms by which MCU inhibition impairs migration remain unknown. While incompletely studied in VSMC, data in neurons and cardiac myoblasts suggest that mitochondrial mobility is reduced when local $Ca^{2+}$ concentrations are high[19]. Therefore, abrogation of MCU activity may lead to local increase in $Ca^{2+}$ concentrations in the vicinity of MCU-deficient mitochondria and thereby, decrease cell migration via arresting mitochondrial mobility.

Emerging studies have suggested that CaMKII, a coordinator of $Ca^{2+}$ handling in multiple cell types, resides within the mitochondrial matrix of cardiac myocytes[20] and lung epithelial cells[21]. Mitochondrial CaMKII has been suggested to regulate MCU in cardiomyocytes, though the data are controversial[20,22,23]. Herein we test the hypothesis that CaMKII in mitochondria of VSMC controls mitochondrial $Ca^{2+}$ uptake and thereby mitochondrial mobility and MCU-dependent VSMC migration, ultimately contributing to neointimal hyperplasia.

## MATERIALS AND METHODS

### Materials

The detailed usage of materials and antibodies are included in the Supplemental Material and Major Resource Tables.

### Mice

All protocols were approved by the University of Iowa Institutional Animal Care and Use Committee and in compliance with the standards for the care and use of laboratory animals of the Institute of Laboratory Animal Resource, National Academy of Science. Mice were maintained in the University of Iowa Animal Facility and treated in accordance with Institutional Animal Care and Use Committee guidelines (PHS Animal Welfare Assurance, A3021-01).

Mice with tamoxifen-inducible Cre recombinase (driven by the SMMHC-promoter) on a C57BL/6 background were used (SM-Cre)[24]. These mice carry the Cre gene on the Y chromosome; hence only male mice were used. HA-tagged mtCaMKIIN mice were generated as previously described[21]. Double-transgenic mice with VSMC-specific expression of mtCaMKIIN (SM-mtCaMKIIN mice) were generated by crossing SM-Cre mice with HA-tagged mtCaMKIIN mice, as diagrammed in Supplemental Figure X A. All mice were genotyped as we previously described[21]. All studies used tamoxifen-treated SM-Cre mice as littermate controls (WT).

Smooth muscle-specific expression of mtCaMKIIN was induced in 6- to 8-week-old male mice via injection of tamoxifen (20 mg/mL, i.p., for 5 days). Recombination was verified by detection of the HA tag in aortic lysates by immunoblot, and by immunofluorescence in 10-

μm frozen carotid sections. Sections were imaged using a Zeiss LSM 510 confocal microscope.

MCU$^{-/-}$ mice in CD1 background were a kind gift of Dr. Toren Finkel (NIH), Miro-1$^{fl/fl}$ mice were graciously provided by Dr. Janet Shaw (Univ. of Utah). Information on strains and sources are provided in the Major Resources Table.

### Vascular smooth muscle cell culture

Primary vascular smooth muscle cells were isolated from aortas and cultured in DMEM (Gibco, #11885-092) supplemented with 10% fetal bovine serum (FBS), 100 U/ml penicillin, 100 μg/ml streptomycin, 8 mM HEPES, MEM vitamins, and non-essential amino acids at 37°C in a humidified 95% air and 5% $CO_2$ incubator[25]. VSMC at passages 4–10 were used for all experiments.

### Adenoviral transduction

VSMC were incubated with adenoviruses expressing mtCaMKIIN, mtGFP, or control at a multiplicity of infection (MOI) of 50 in serum-free media overnight. Subsequent experiments were conducted 48–72 h after adenoviral transduction as described previously[21]. Miro-1$^{-/-}$ were generated by infecting VSMC from Miro$^{fl/fl}$ mice with adenovirus expressing cre recombinase at MOI of 10[26]. Deletion of Miro-1 was confirmed 72 hours after infection by immunoblot.

### Isolation of mitochondrial fractions and mitoplasts

Cleaned, segmented mouse aortas or cultured VSMC were suspended in MSE (5 mM 3-(N-morpholino)propanesulfonic acid, 70 mM sucrose, 2 mM ethyleneglycol-*bis*-(β-aminoethyl ether)-*N,N′*-tetraacetic acid, 220 mM mannitol, pH 7.2, with KOH) on ice followed by homogenization by mortar and pestle. Nuclei and unbroken cells were pelleted by centrifugation at 600 × *g* for 10 min. Then, centrifugation of the supernatant at 8,500 × *g* for 20 mins separated crude mitochondrial from cytosolic fractions. The mitochondrial pellet was resuspended in MSE with protease inhibitors. For mitoplast preparations, crude mitochondria were digested in 20 nM Proteinase K in MSE for 5 minutes on ice. The reaction was stopped by adding PMSF (1 mM), and mitoplasts were pelleted at 10,000×*g* for 10 min and resuspended in MSE with protease inhibitors.

### Immunoblotting

Immunoblotting experiments were performed following the general protocol for western blotting by BioRad and detailed protocol in the Supplemental Materials. Equivalent amounts of protein of were separated by SDS/PAGE on 4–20% Tris/glycine gels (BioRad) and transferred to PVDF membranes. Blots were scanned and analyzed using ImageJ.

### Determination of mitochondrial $Ca^{2+}$

Ratiometric $Ca^{2+}$ measurements in mitochondria were performed in VSMC after transduction with adenovirus expressing mtPericam (Ad-mtPericam)[27]. Pericam ratiometric fluorescent imaging with the Leica SP8 STED imaging system was used to determine fluorescence signal intensity, with an excitation at 405nm/480nm and acquisition at 510nm.

Real-time Pericam fluorescence ratios were recorded after addition of PDGF. Peak amplitude (R) was calculated by subtracting the baseline fluorescence ratio from the highest fluorescence ratio. The area under the curve (AUC) from baseline was determined using GraphPad Prism. Summary data represent the average difference in basal and peak mitochondrial [$Ca^{2+}$].

The o-Cresolphthalein conjugation colorimetric plate assay was used to measure $Ca^{2+}$ concentration of isolated mitochondria from thoracic aortas or cultured VSMC. Mitochondrial $Ca^{2+}$ was assessed per the manufacturer's protocol (Cayman Scientific) and normalized to total mitochondrial protein concentration.

### Determination of cytosolic $Ca^{2+}$ transients

Cells were loaded with 2 μM Fura-2 acetoxymethyl ester (Fura-2AM) $Ca^{2+}$-free HBSS for 20 min at 25°C, then washed with $Ca^{2+}$-containing HBSS at 37° for 20 min. Cells were excited alternatively at 340 and 380 nm. Fluorescence signal intensity was acquired at 510 nm. Real-time shifts in Fura-2AM fluorescence ratio were recorded as PDGF was acutely added using Olympus IX81 Inverted Light Microscope. Peak amplitude (R) was calculated by subtracting the baseline fluorescence ratio from the highest fluorescence ratio. Summary data was calculated using GraphPad Prism.

### Migration assays

Boyden chamber and traditional scratch wound assays were performed as previously described and detailed in the Supplemental Material[28]. To perform high throughput migration assays, VSMC were grown to confluence in a 96-well Black, Clear Bottom, Tissue Culture 96-Well with Lid (Perkin Elmer #6005550). Wounding was performed by inserting a conical 96-well PCR plate and scraping to create a cell-free zone. Cells were washed with DMEM and treated in DMEM containing PDGF or vehicle control. Images were taken at 10× at 0 – 48 hr after injury using the Perkin Elmer Operetta High-Content Imaging System by Digital Phase Contrast (DPC). Semi-automated analysis was performed using Image J as detailed in Supplemental Figure III. Each condition was performed and analyzed in quadruplicate for each independent experiment.

### Quantification of mitochondrial distribution

To visualize mitochondrial distribution in migrating cells, VSMC were simultaneously infected with Ad-mtGFP and Ad-control or Ad-mtCaMKIIN. Cells were subject to a scratch wound assay and allowed to migrate in DMEM/10% FBS and PDGF for indicated time points. Inhibitors for mitochondria $Ca^{2+}$ (Ru360, 1μM), mtROS (mitoTEMPO, 10μM), actin polymerization (Cytochalasin D, 0.1nM) and microtubules (Nocodazole, 1μM) were given for the duration of migration. For some experiments, VSMC with Nocodazole were washed and left in DMEM/10% FBS 2 hr prior to fixation to allow microtubule re-polymerization. VSMC were then fixed and stained with phalloidin 568. Images were acquired using a Zeiss 510 confocal microscope with a 40× objective. Mitochondrial distribution was quantified using NIH ImageJ by line scan of mitochondria from the nucleus to the leading edge and by region of interest at the leading edge as outlined in detail in Supplemental Figure V. For both methods, data are expressed as percent of mitochondria in the leading edge area or segment.

The image analysis was performed independently by two scientists who were blinded to the treatment group.

### Focal adhesion immunostaining and analysis

VSMC infected with Ad-control or Ad-mtCaMKIIN, were grown to confluence on glass coverslips. A scratch wound assay was performed with PDGF. After 6 hr, cells were washed and fixed in 4% PFA, then subject to the staining protocol described in the supplemental detailed methods. Cells were stained with anti-vinculin primary antibody and phalloidin-568. Images were acquired using the Zeiss LSM 510 confocal microscope. Confocal images were thresholded equally across experiments by ImageJ. Region of interest (ROI) was selected at the leading edge of every cell and “Analyze Particles” function was used to identify and measure all FA.

### Focal Adhesion Turnover

VSMC were nucleofected with GFP-Vinculin plasmid. Images of labeled FA in VSMC were taken after addition of DMEM/10% FBS containing PDGF every 15 minutes for a total of 90 minutes. Imaging was performed using the custom-built Nikon BX-81 microscope at 40× objective. Images were automatically thesholded by CellProfiler and FA were identified by “Primary Objects” function. The first image (green) and last image (red) were pseudocolored and overlayed in CellProfiler. Colocalization of green and red signal of FA at times 0 min and 90 min was expressed by Mander’s coefficient.

### Carotid injury model

Male mice (10–12 weeks-old) were subject to carotid injury by endothelial denudation using a resin-bead coated suture as described in the Supplemental Materials[29]. At 28 days after injury, all animals were anesthetized and perfused with PBS followed by 4% PFA for 3 min. The carotid arteries were excised and paraffin-embedded. Carotid artery cross sections (5 μm) were obtained at 50 μm intervals from the carotid bifurcation site for up to 500 μm and stained by Verhoeff’s Van Gieson. Luminal and intimal areas were determined by tracing the circumference of the internal elastic lamina (IEL), and the luminal area using NIH Image J. The neointimal area was calculated by subtracting the luminal area from the IEL area.

### Nucleofection

Cells were nucleofected, following manufacturer’s protocol (Lonza #VPI-1004). Briefly, 600,000 cells were nucleofected in the presence of 5 μg plasmid DNA and plated onto 3 cm glass coverslip dishes. For focal adhesion turnover assays, VSMC were infected with either Ad-mtCaMKIIN or Ad-Control the next day and allowed to express for 48 hour.

### Statistical Analyses

Data are expressed as mean±SEM and analyzed with GraphPad Prism 7.0 software. All data sets were analyzed for normality and equal variance. Kruskall-Wallis test with Dunn’s post hoc test was used for data sets where normal distribution could not be assumed. Two-tailed unpaired Student’s T-test and 1-way ANOVA followed by Tukey’s multiple comparison test were used for data sets with normal distribution. Two-way ANOVA followed by Tukey’s

multiple comparison test was used for grouped data sets. A p-value < 0.05 was considered significant.

## RESULTS

### CaMKII is present and active in mitochondria of VSMC

We first established that CaMKII is present in mitochondria of VSMC. We detected CaMKII in whole mitochondria and in mitoplasts, mitochondrial preparations that contain only the matrix and inner mitochondrial membrane (Figure 1A). Next, we tested whether CaMKII in mitochondria is activated by PDGF, a well-established agonist in VSMC migration and neointimal hyperplasia[30]. PDGF increased the $Ca^{2+}$/calmodulin-dependent autophosphorylation of CaMKII at Thr-287 in particular in mitoplasts (Figure 1B).

Since CaMKII is activated by $Ca^{2+}$/CaM binding and subsequent autophosphorylation, we examined whether deletion or inhibition of the mitochondrial $Ca^{2+}$ influx channel MCU alters PDGF-induced activation of CaMKII in mitochondria (mtCaMKII). Deficiency of MCU or inhibition of MCU with the pharmacologic inhibitor Ru360 abrogated mtCaMKII activation in mitoplasts (Figure 1B, Supplementary Figure IA). Phosphorylation of MCU at S92, a highly conserved site on the N-terminal domain of MCU, is essential for mitochondrial $Ca^{2+}$ uptake[15]. Thus, we overexpressed WT MCU and a mutant of MCU that cannot be phosphorylated at S92 (S92A) in $MCU^{-/-}$ VSMC (Figure 1C). Whereas WT MCU expression restored the phosphorylation of CaMKII, this effect was absent with mutant MCU. Of note, we confirmed that expression of MCU WT, but not of the MCU S92A mutant in $MCU^{-/-}$ markedly augmented mitochondrial $Ca^{2+}$ uptake (data not shown). These data suggest that $Ca^{2+}$ influx via MCU is necessary and sufficient for CaMKII activation in mitoplast of VSMC.

Studies in other cell types have suggested that mtCaMKII phosphorylates MCU at S92 although direct evidence is currently missing[15]. To test the effects of mtCaMKII, we developed a model of mitochondrial CaMKII inhibition by adenoviral delivery of CaMKIIN, a specific peptide that blocks substrate binding to all CaMKII isoforms[31]. A COX8 mitochondrial targeting sequence was used to target CaMKIIN to the mitochondrial matrix (mtCaMKIIN). In immunoblots, we confirmed mtCaMKIIN expression in mitoplasts, with minimal detection in the cytosol (Supplemental Figure IB, C). Using immunoblots for activated ERK1/2, a bona fide cytosolic CaMKII signaling target[30,32] we excluded additional cytosolic effects of mtCaMKIIN (Supplemental Figure ID). To provide direct evidence that mtCaMKII regulates MCU phosphorylation, we utilized an antibody that specifically detects phosphorylation of S92 on MCU (Supplemental Figure IE). In isolated mitochondria of WT cells, PDGF induced phosphorylation of MCU, which was abrogated with mtCaMKIIN expression at baseline and after PDGF (Figure 1D). Taken together with the data demonstrating that MCU is necessary for mtCaMKII activation, our findings support a feed-forward circuit by which mitochondrial $Ca^{2+}$ uptake via MCU activates mtCaMKII that phosphorylates MCU at S92 and further augments mitochondrial $Ca^{2+}$ influx.

Therefore, we sought to confirm that mtCaMKII inhibition decreases mitochondrial $Ca^{2+}$ uptake using the ratiometric mitochondria-targeted $Ca^{2+}$ indicator protein Pericam (mtPericam)[33]. PDGF induced mitochondrial $Ca^{2+}$ uptake, and mtCaMKIIN significantly blunted the increase in $Ca^{2+}$ after PDGF treatment (Figure 1E). Moreover, the peak amplitude of the $Ca^{2+}$ signal and the area under the curve were reduced (AUC, Figure 1E). Accordingly, we observed significantly lower mitochondrial $Ca^{2+}$ levels in VSMC with mtCaMKIIN expression compared to control-infected cells based on $Ca^{2+}$ complex formation with O-Cresolphthalein (Figure 1F). To further interrogate the regulatory circuit between mtCaMKII and MCU, we measured mitochondrial $Ca^{2+}$ uptake in $MCU^{-/-}$ VSMC. Overexpression of mitochondria-targeted CaMKII in WT VSMC was sufficient to augment PDGF-induced mitochondrial matrix $Ca^{2+}$ uptake (Figure 1G, Supplemental Figure IF). MCU was necessary for the effect since the $Ca^{2+}$ influx was completely abrogated in MCU −/− VSMC with mtCaMKII overexpression (Figure 1G). These data further support the presence of a feed-forward mtCaMKII and MCU.

To determine whether other agonists that also increase cytoplasmic $Ca^{2+}$ levels have an effect on CaMKII activation in mitochondria, we confirmed our findings using histamine stimulation. Specifically, histamine promoted CaMKII phosphorylation in mitoplasts (Supplemental Figure IG), and treatment with mtCaMKIIN blunted mitochondrial $Ca^{2+}$ uptake (Supplemental Figure IH). These data support that mitochondrial CaMKII activation is a general mechanism in mitochondrial $Ca^{2+}$ uptake.

## Inhibition of mitochondrial $Ca^{2+}$ uptake prevents VSMC migration

We next tested whether inhibition of mitochondrial CaMKII is sufficient to alter VSMC phenotypes. mtCaMKIIN had no significant effect on cell counts following agonist stimulation (Supplemental Figure IIA), where as VSMC migration was profoundly inhibited by mtCaMKIIN in Boyden chamber migration (Figure 2A) or wounding assays (Figure 2B). These findings were confirmed using siRNA-mediated MCU silencing (Supplemental Figure IIB, C).

To overcome the limitations of conventional migration assays, we developed a novel high-throughput scratch wound migration assay with semi-automated data analysis (Supplemental Figure IIIA). mtCaMKIIN blocked PDGF-induced VSMC migration in a dose-dependent manner at 24 hours after scratch wound in the presence of a proliferation inhibitor (Figure 2C, D). Of note, mtCaMKII overexpression in WT VSMC moderately increased VSMC migration (Figure 2E).

As anticipated, PDGF-induced migration of VSMC from $MCU^{-/-}$ mice was significantly impaired using the high throughput scratch wound migration assay (Figure 2F). Expression of mtCaMKIIN or mtCaMKII in $MCU^{-/-}$ VSMC had no significant additional effect on VSMC migration (Figure 2F). As a separate strategy for MCU inhibition, we examined increasing concentrations of the MCU inhibitor Ru360. As expected, we observed a dose-response to Ru360 (Supplemental Figure IIIB). Under mtCaMKII overexpression, higher doses of Ru360 were required to delay would closure. These data support that mitochondrial $Ca^{2+}$ uptake via MCU is necessary for the action of mitochondrial CaMKII on VSMC migration.

In addition to mitochondrial $Ca^{2+}$ uptake, both mitochondrial metabolism and mitochondrial ROS production have been implicated in cell migration. We measured oxygen consumption (OCR), an indicator of mitochondrial respiration, following PDGF treatment and did not observe appreciable differences with expression of mtCaMKIIN (Supplemental Figure IVA). Next, we tested the effect of mtCaMKII inhibition or overexpression on mitochondrial ROS generation. As anticipated, mtCaMKII promoted while mtCaMKIIN abolished PDGF-induced mitochondrial ROS production (Supplemental Figure IVB, C). Treatment with the mitochondrial ROS scavenger mitoTEMPO attenuated migration in mtCaMKII-expressing VSMC, but did not alter migration in cells expressing mtCaMKIIN (Supplemental Figure IVD). These data are consistent with the concept of mitochondrial $Ca^{2+}$ uptake via mtCaMKII as an upstream regulator of mitochondrial ROS production.

## Mitochondrial CaMKII inhibition blocks mitochondrial translocation towards the leading edge

Studies in non-vascular cells demonstrate that mitochondrial translocation to the leading edge is required for cell migration[7,9,10]. In growth-arrested VSMC, mitochondria were predominantly localized in the perinuclear area (Figure 3A). PDGF treatment of WT VSMC for 6–12 hr after scratch wound induced mitochondrial translocation to the anterior edge (Figure 3A, B, Supplemental Figure V), providing evidence that mitochondrial mobility occurs in migrating VSMC. In contrast, mtCaMKIIN significantly inhibited the PDGF-induced mitochondrial redistribution at 6–24 hr (Figure 3C). This effect was phenocopied in $MCU^{-/-}$ VSMC or by Ru360 (Figure 3C). While we found that mtCaMKIIN reduced mitochondrial ROS production, treatment of WT VSMC with mitoTEMPO had no effect on redistribution of mitochondria to the leading edge (Figure 3C). We also tested whether acute MCU inhibition with Ru360 could arrest translocating mitochondria in migrating WT VSMC. Indeed, when Ru360 was added at 6 hr after initiation of migration with PDGF, further mitochondrial redistribution was prevented (Supplemental Figure VI). Together, these data suggest that inhibition of mitochondrial $Ca^{2+}$ uptake arrests mitochondrial translocation.

To provide direct experimental evidence that mitochondrial translocation is $Ca^{2+}$-dependent, we expressed WT MCU and the MCU S92A mutant with decreased mitochondrial $Ca^{2+}$ influx in $MCU^{-/-}$ VSMC. Whereas WT MCU recovered VSMC migration and mitochondrial translocation to the leading edge, MCU mutant S92A did not, confirming that mitochondrial mobility depends on mitochondrial matrix $Ca^{2+}$ uptake (Figure 3D, E).

## Miro-1 is required for mtCaMKII-mediated active mitochondrial translocation in VSMC

Mitochondria rely on intact cytoskeletal proteins to efficiently traffic throughout the cell. We tested whether mitochondrial mobility in migrating cells is an active process or whether it passively follows cell movement. We treated cells with either a microtubule or an actin inhibitor, both of which arrest cell migration[34,35]. Only the microtubule inhibitor, nocodazole, prevented mitochondrial mobility to the leading edge (Figure 4A), suggesting that mitochondrial translocation in migrating cells is an active process that is selectively regulated by microtubule dynamics. In addition, PDGF treatment of contact-inhibited, confluent VSMC promoted redistribution of mitochondria away from the nucleus to the cell

periphery (Supplemental Figure VII A), further substantiating that mitochondrial mobility is not a passive event.

Precedence for active mitochondrial motility comes from studies in neurons that identified the outer mitochondrial membrane GTPase Miro-1 as a coordinator of mitochondrial translocation along microtubules[36]. Upon $Ca^{2+}$ binding to the two EF hands of Miro-1, mitochondria and microtubules dissociate, which induces mitochondrial arrest. Thus, we isolated aortic VSMC from Miro-$1^{fl/fl}$ mice and induced Miro-1 deletion by cre recombination (Miro-$1^{-/-}$, Figure 4B). In Miro-$1^{-/-}$ VSMC, we detected mitochondrial arrest and strongly impaired VSMC migration in the presence of PDGF (Figure 4C–E). Overexpression of mtCaMKII or mtCaMKIIN had no effect on mitochondrial translocation or VSMC migration in Miro-$1^{-/-}$ VSMC. Similar results were obtained by overexpressing wild-type MCU or a dominant negative mutant that decreases the $Ca^{2+}$ influx[37] in Miro-$1^{-/-}$ VSMC (Supplemental Figure VII B, D). These data demonstrate that in VSMC, Miro-1 is necessary for migration and mitochondrial translocation to the leading edge.

Mitochondrial mobility is abrogated by increases in local 'peri-mitochondrial' $Ca^{2+}$ levels[36]. Since we observed a significant reduction in mitochondrial $Ca^{2+}$ uptake with MCU or mtCaMKII inhibition, we examined their impact on cytosolic $Ca^{2+}$ transients using the ratiometric indicator Fura-2AM. Expression of mtCaMKIIN did not alter baseline cytosolic $Ca^{2+}$ levels (data not shown). Whereas total cytosolic $Ca^{2+}$ levels were transiently increased in control-infected cells following PDGF treatment, the decay of the cytosolic $Ca^{2+}$ signal was significantly prolonged under mtCaMKII inhibition, as evidenced by greater tau ($\tau$), residual amplitude, and AUC (Figure 4F). Together with the data in Figure 1, these findings suggest that mtCaMKII inhibition prevents mitochondrial matrix $Ca^{2+}$ uptake and thereby prolongs the PDGF-induced transient increases in total cytosolic $Ca^{2+}$. We posit that the perturbed cytosolic $Ca^{2+}$ transients by mtCaMKII inhibition disrupt Miro-1-dependent mitochondrial translocation towards the leading edge and arrest migration of VSMC.

Since VSMC with small, fragmented mitochondria are reported to have a higher propensity to migrate[4], we assessed mitochondrial morphology[38]. In accordance with published evidence[39], PDGF induced mitochondrial fission in control-infected VSMC (Supplemental Figure VIII). With mtCaMKII inhibition, mitochondria were fragmented at baseline without further change in morphology with PDGF.

## Mitochondrial CaMKII-dependent mitochondrial translocation is necessary for focal adhesion dynamics

Mitochondria provide the energy source for dynamic focal adhesion (FA) turnover at the leading edge, which is necessary for cell migration[10,40]. Since mtCaMKIIN prevented mitochondrial translocation to the leading edge, we next interrogated the effect of mtCaMKII inhibition on FA dynamics. We first assessed FA turnover by time-lapse imaging after scratch wounding and PDGF treatment. Here, mtCaMKIIN prevented the dynamic changes in FA redistribution observed in control-infected VSMC after 90 min (Figure 5A). We also assessed FA size as a surrogate for FA turnover since FA size predicts cell migration[41]. In migrating VSMC, FA size was decreased after PDGF treatment (Figure 5B).

Conversely, mtCaMKIIN-expressing VSMC exhibited large, stable FA, suggesting that mtCaMKII inhibition promotes static FA associated with reduced cell migration.

In addition, we analyzed phosphorylation of focal adhesion kinase (FAK) at Y577 as a marker for FA activity[42]. As compared to control-infected cells, the phosphorylation was reduced in VSMC expressing mtCaMKIIN (Figure 5C). MLC inserts at the vicinity of FA and is phosphorylated to coordinate forward migration forces[43]. Accordingly, colocalization of pMLC to FA was reduced in VSMC expressing mtCaMKIIN compared to controls (Supplemental Figure IX). These data suggest that, under mtCaMKII inhibition, reduced localization of mitochondria to the leading edge depletes the energy source necessary for dynamic FA turnover.

### Mitochondrial CaMKII inhibition ameliorates neointimal hyperplasia in an in vivo model of endothelial injury

To test whether mtCaMKII inhibition reduces neointimal hyperplasia in vivo, we engineered a novel transgenic mouse model with inducible, smooth muscle-specific mtCaMKIIN expression (termed “SM-mtCaMKIIN” mice, Supplemental Figure XA). We confirmed robust transgene expression by qrtPCR and immunofluorescent staining of mtCaMKIIN in the carotid media after tamoxifen-induced cre activation (Supplemental Figure XB, Figure 6A). Immunoblots of cytosolic and mitochondrial fractions confirmed the presence of the transgene predominantly in mitochondria (Figure 6B). Functional mtCaMKII inhibition was confirmed by a decrease in mitochondrial $Ca^{2+}$ concentration (Figure 6C).

Next, we performed vascular injury by endothelial denudation of the left common carotid artery. On day 28 after endothelial injury, the neointimal area in SM-mtCaMKIIN mice was significantly reduced compared to littermate controls (Figure 6D, Supplemental Figure XE). In uninjured right carotid arteries, there was no apparent difference in arterial morphology with mtCaMKIIN expression (Figure 6D).

To examine the translational potential of our findings, we performed co-immunostaining for CaMKII and a mitochondrial marker in human coronary arteries from autopsy samples (Supplemental Figure XF). 3D projections of z-stack images demonstrated colocalization of mitochondria and CaMKII in the intima. Most CaMKII-positive cells in areas of subintimal thickening also expressed smooth muscle actin.

## Discussion

The goal of this study was to identify key regulators of mitochondrial function that contribute to VSMC migration and neointimal hyperplasia. First, we demonstrate that CaMKII resides in mitoplasts of VSMC and was activated by PDGF. Activation of CaMKII in mitochondria was abrogated when MCU was deleted. Inhibition of mtCaMKII lowered the phosphorylation of MCU at S92, a site that is crucial for mitochondrial $Ca^{2+}$ uptake by MCU activity. MtCaMKII inhibition blocked mitochondrial translocation to the leading edge and VSMC migration. These effects were recapitulated by deletion of MCU. Overexpression of WT MCU but not of the MCU mutant S92A in $MCU^{-/-}$ VSMC recovered mitochondrial translocation and migration, suggesting that the effects of MCU or mtCaMKII on these

phenotypes are caused by altered mitochondrial $Ca^{2+}$ uptake. $Ca^{2+}$-dependent mitochondrial mobility is coordinated by Miro-1, an outer mitochondrial membrane GTPase. In agreement, in Miro-$1^{-/-}$ VSMC, mitochondrial mobility and migration were abolished, establishing Miro-1 as a key regulator of mitochondrial function in VSMC. mtCaMKII overexpression or inhibition did not have any effect in Miro-$1^{-/-}$ VSMC, suggesting that Miro-1 mediates the effect of mtCaMKII on mitochondrial mobility and migration. Consistent with the notion that increased $Ca^{2+}$ levels arrest mitochondria, $Ca^{2+}$ clearance from the cytosol was delayed with mtCaMKII inhibition. Moreover, mtCaMKII inhibition led to impaired FA turnover and phosphorylation of cytoskeletal proteins necessary for coordinated anterior cell movement. In agreement with in vitro findings, transgenic CaMKII inhibition selectively in mitochondria of VSMC significantly reduced neointimal hyperplasia after endothelial vascular injury. Together these data provide key mechanistic insight into how mitochondrial function regulates VSMC migration and neointimal hyperplasia: mtCaMKII controls mitochondrial $Ca^{2+}$ uptake through activation of MCU and is necessary for mitochondrial translocation to the leading edge of migrating VSMC where mitochondria support FA and cytoskeletal remodeling (Figure 6E).

Several other studies support that mitochondrial $Ca^{2+}$ uptake regulates cell migration[17]. For example, MCU inhibition or knockdown halts cell migration of cancer cells, whereas increased expression of MCU correlates with an invasive phenotype[16]. Our data in VSMC are in line with these observations and provide further insight into how regulation of mitochondrial $Ca^{2}$ uptake is regulated and affects VSMC migration. CaMKII has been detected in the mitochondrial matrix of cardiac myocytes and reported to blunt mitochondrial matrix $Ca^{2+}$ uptake[20]. Here, we provide further mechanistic evidence for the actions of mtCaMKII in mitochondria; phosphorylation of MCU at S92, a validated strong regulatory site for MCU activity[15], was reduced when mtCaMKII activity is inhibited. CaMKII activation requires an initial binding of calcified calmodulin that is abundant in the mitochondrial matrix[44]. Accordingly, mtCaMKII activation was abrogated when MCU was deleted or inhibited. Moreover, mtCaMKII inhibition prevented further mitochondrial $Ca^{2+}$ uptake, suggesting a feed forward circuit in which initial mitochondrial $Ca^{2+}$ influx via MCU is required for mtCaMKII activation, which in turn controls MCU activity via phosphorylation at S92. mtCaMKII thereby drives further mitochondrial $Ca^{2+}$ uptake. Alternatively, mtCaMKII may regulate $Ca^{2+}$ uptake via phosphorylation of other sites on MCU, such as S57 as proposed by a recent study, phosphorylation of MCU regulators MICU or EMRE[14,45], or potentially by activating $Ca^{2+}$ influx via another $Ca^{2+}$ channel, such as the mitochondrial RyR receptor[46].

Previous studies reported that dynamic mitochondrial fission and fusion are required for VSMC migration. In particular, migration was abolished when a dominant negative mutant of Drp-1, a master regulator of mitochondrial fission, was expressed in VSMC. Based on this study and other reports, it has been proposed that VSMC with small, fragmented mitochondria have a higher propensity to migrate[4]. However, with mtCaMKII inhibition, mitochondria were fragmented at baseline without further change in morphology with PDGF, implying that mitochondrial size is not a major determinant of mobility when mitochondrial $Ca^{2+}$ uptake is altered. Our study provides novel mechanistic insight by defining mitochondrial mobility as a function of $Ca^{2+}$ levels and a prerequisite for VSMC

migration and likely neointimal hyperplasia. Mitochondrial mobility is arrested in microdomains of high $Ca^{2+}$ concentrations, as may occur in the vicinity of mitochondrial/ER convergence zones when the mitochondrial $Ca^{2+}$ uptake is impaired with MCU or mtCaMKII inhibition. In subcellular domains of high $Ca^{2+}$ concentrations in neurons[19,36], $Ca^{2+}$ binding to the EF hands of the Rho-GTPase Miro-1 induces the dissociation of mitochondria from microtubules, followed by mitochondrial arrest. Our findings are in agreement with these data and demonstrate that mitochondrial translocation in VSMC is an active process and controlled by Miro-1. Alternatively, tethering of mitochondria to actin filaments via myosin V, which is induced by locally increased $Ca^{2+}$ levels, has been implicated to halt mobile mitochondria[47]. However, our data do not support this mechanism since we detected mitochondrial redistribution to the leading edge despite disruption of the actin cytoskeleton. Once at the leading edge, mitochondria cluster in the vicinity of FA, in order to meet the significant energy demands for FA turnover and cytoskeletal remodeling in migrating cells[7,10,11,40]. Consistent with this mechanism, we detected reduced FA activity under mtCaMKII inhibition.

CaMKII is well accepted to be present and active in the cytosol and nucleus where it fulfills distinct roles in the regulation of transcriptional events[48,49] substrate phosphorylation of a wide array of signaling mediators[50]. Different approaches to “globally” block intracellular CaMKII activity have revealed its regulatory function in cell migration. Using a mitochondria-targeted CaMKII inhibitory peptide, we discovered that the effects of CaMKII on migration are due, at least in part, to its actions in mitochondria. Previous data suggest that the spatial and functional specificity in CaMKII activation is elicited by mobilization of different $Ca^{2+}$ stores[50]. Thus, inhibiting mtCaMKII activity may be sufficient to block cell migration regardless of its actions in other cellular compartments. The CaMKII isoform(s) that are present or predominant in mitochondria are currently unknown. However, our approach of overexpressing an inhibitor that blocks all isoforms overcomes this obstacle.

Mitochondria-derived ROS promotes VSMC migration[4]. Here, we found that mtCaMKII inhibition diminished mitochondrial ROS production, in line with previous data for MCU[51]. Mitochondrial $Ca^{2+}$ uptake is a prerequisite for ROS production in mitochondria, for example by increasing Krebs cycle activity and substrate delivery to the electron transport chain[12]. Therefore, we consider mtCaMKII as a regulator of these upstream metabolic events leading to mitochondrial ROS production. Mitochondrial translocation to the leading edge was not altered in VSMC pretreated with a mitochondrial ROS scavenger, suggesting that mitochondrial ROS production in itself promotes migration through additional pathways, likely related to redox signaling[52].

Together, this study identifies mtCaMKII as an important regulator of MCU and mitochondrial $Ca^{2+}$ uptake and provides evidence that mitochondrial $Ca^{2+}$ uptake promotes VSMC migration via control of mitochondrial mobility. The data presented here also synthesize several disparate concepts introduced in the literature. First, mitochondrial $Ca^{2+}$ uptake determines cytosolic $Ca^{2+}$ transients[53,54], high cytosolic $Ca^{2+}$ arrests mitochondrial mobility[36], which in turn determines cell migration[10]. Moreover, our results link mtCaMKII and mitochondrial $Ca^{2+}$ uptake with a recent report demonstrating that mitochondria colocalize to focal adhesions to maintain the subcellular energy demands of structural

remodeling in cell migration[40]. Future work focusing on regulators of mitochondrial mobility may reveal novel therapeutic options to mitigate neointimal hyperplasia after vascular injury.

## Supplementary Material

Refer to Web version on PubMed Central for supplementary material.

## Acknowledgments

The authors thank Dr. Kris DeMali (University of Iowa) for the kind gift of the GFP-Vinculin plasmid and Dr. Janet Shaw (University Utah and HHMI) for Miro-$1^{fl/fl}$ mice.

**Sources of Funding**: The project was supported by grants from the NIH (R01 HL 108932 to IMG); the Veterans Affairs Iowa City (I01 BX000163 to IMG), the American Heart Association (14SDG18850071 to WHT, 17GRNT33660032 to IMG) and from the NIH NHLBI (F30 HL131078-01, T32 GM007337 to EKN).

## ABBREVIATIONS

| | |
|---|---|
| **DN-MCU** | Dominant Negative Mitochondrial Calcium Uniporter |
| **FA** | Focal Adhesion |
| **PDGF** | Platelet Derived Growth Factor |
| **FAK** | Focal Adhesion Kinase |
| **MCU** | Mitochondrial Calcium Uniporter |
| **Miro-1** | Rho-GTPase responsible for mitochondrial mobility |
| **mitoTEMPO** | mitochondrial reactive oxygen species scavenger |
| **MLC** | Myosin Light Chain |
| **mtCaMKII** | $Ca^{2+}$/Calmodulin-dependent Kinase II in mitoplast |
| **mtCaMKIIN** | mitochondrially targeted peptide inhibitor of CaMKII |
| **mtROS** | mitochondrial reactive oxygen species |
| **Ru360** | pharmacologic inhibitor of MCU |
| **VSMC** | vascular smooth muscle cell |

## References

1. Moses JW, Leon MB, Popma JJ, Fitzgerald PJ, Holmes DR, O'Shaughnessy C, Caputo RP, Kereiakes DJ, Williams DO, Teirstein PS, Jaeger JL, Kuntz RE. Investigators S. Sirolimus-eluting stents versus standard stents in patients with stenosis in a native coronary artery. The New England journal of medicine. 2003; 349:1315–1323. [PubMed: 14523139]
2. Schwartz SM. Perspectives series: cell adhesion in vascular biology. Smooth muscle migration in atherosclerosis and restenosis. The Journal of Clinical Investigation. 1997; 99:2814–2816. [PubMed: 9185501]

3. Wang JN, Shi N, Chen SY. Manganese superoxide dismutase inhibits neointima formation through attenuation of migration and proliferation of vascular smooth muscle cells. Free Radic Biol Med. 2012; 52:173–181. [PubMed: 22062629]

4. Wang L, Yu T, Lee H, O'Brien DK, Sesaki H, Yoon Y. Decreasing mitochondrial fission diminishes vascular smooth muscle cell migration and ameliorates intimal hyperplasia. Cardiovasc Res. 2015; 106:272–283. [PubMed: 25587046]

5. Madamanchi NR, Runge MS. Mitochondrial dysfunction in atherosclerosis. Circ Res. 2007; 100:460–473. [PubMed: 17332437]

6. Dikalov SI, Ungvari Z. Role of mitochondrial oxidative stress in hypertension. Am J Physiol Heart Circ Physiol. 2013; 305:H1417–1427. [PubMed: 24043248]

7. Cunniff B, McKenzie AJ, Heintz NH, Howe AK. AMPK activity regulates trafficking of mitochondria to the leading edge during cell migration and matrix invasion. Molecular Biology of the Cell. 2016; 27:2662–2674. [PubMed: 27385336]

8. Desai Salil P, Bhatia Sangeeta N, Toner M, Irimia D. Mitochondrial Localization and the Persistent Migration of Epithelial Cancer cells. Biophysical Journal. 2013; 104:2077–2088. [PubMed: 23663851]

9. Zhao J, Zhang J, Yu M, Xie Y, Huang Y, Wolff DW, Abel PW, Tu Y. Mitochondrial dynamics regulates migration and invasion of breast cancer cells. Oncogene. 2013; 32:4814–4824. [PubMed: 23128392]

10. Caino MC, Seo JH, Aguinaldo A, Wait E, Bryant KG, Kossenkov AV, Hayden JE, Vaira V, Morotti A, Ferrero S, Bosari S, Gabrilovich DI, Languino LR, Cohen AR, Altieri DC. A neuronal network of mitochondrial dynamics regulates metastasis. Nat Commun. 2016; 7:13730. [PubMed: 27991488]

11. Caino MC, Ghosh JC, Chae YC, Vaira V, Rivadeneira DB, Faversani A, Rampini P, Kossenkov AV, Aird KM, Zhang R, Webster MR, Weeraratna AT, Bosari S, Languino LR, Altieri DC. PI3K therapy reprograms mitochondrial trafficking to fuel tumor cell invasion. Proc Natl Acad Sci U S A. 2015; 112:8638–8643. [PubMed: 26124089]

12. Brookes PS, Yoon Y, Robotham JL, Anders MW, Sheu SS. Calcium ATP, and ROS: a mitochondrial love-hate triangle. Am J Physiol Cell Physiol. 2004; 287:C817–833. [PubMed: 15355853]

13. Poburko D, Lee CH, van Breemen C. Vascular smooth muscle mitochondria at the cross roads of Ca(2+) regulation. Cell Calcium. 2004; 35:509–521. [PubMed: 15110141]

14. Mallilankaraman K, Doonan P, Cardenas C, Chandramoorthy HC, Muller M, Miller R, Hoffman NE, Gandhirajan RK, Molgo J, Birnbaum MJ, Rothberg BS, Mak DO, Foskett JK, Madesh M. MICU1 is an essential gatekeeper for MCU-mediated mitochondrial Ca(2+) uptake that regulates cell survival. Cell. 2012; 151:630–644. [PubMed: 23101630]

15. Lee Y, Min CK, Kim TG, Song HK, Lim Y, Kim D, Shin K, Kang M, Kang JY, Youn HS, Lee JG, An JY, Park KR, Lim JJ, Kim JH, Kim JH, Park ZY, Kim YS, Wang J, Kim DH, Eom SH. Structure and function of the N-terminal domain of the human mitochondrial calcium uniporter. EMBO Rep. 2015; 16:1318–1333. [PubMed: 26341627]

16. Prudent J, Popgeorgiev N, Gadet R, Deygas M, Rimokh R, Gillet G. Mitochondrial Ca(2+) uptake controls actin cytoskeleton dynamics during cell migration. Scientific Reports. 2016; 6:36570. [PubMed: 27827394]

17. Tosatto A, Sommaggio R, Kummerow C, Bentham RB, Blacker TS, Berecz T, Duchen MR, Rosato A, Bogeski I, Szabadkai G, Rizzuto R, Mammucari C. The mitochondrial calcium uniporter regulates breast cancer progression via HIF-1alpha. EMBO Mol Med. 2016; 8:569–585. [PubMed: 27138568]

18. Tang S, Wang X, Shen Q, Yang X, Yu C, Cai C, Cai G, Meng X, Zou F. Mitochondrial Ca(2)(+) uniporter is critical for store-operated Ca(2)(+) entry-dependent breast cancer cell migration. Biochem Biophys Res Commun. 2015; 458:186–193. [PubMed: 25640838]

19. Yi M, Weaver D, Hajnoczky G. Control of mitochondrial motility and distribution by the calcium signal: a homeostatic circuit. J Cell Biol. 2004; 167:661–672. [PubMed: 15545319]

20. Joiner ML, Koval OM, Li J, He BJ, Allamargot C, Gao Z, Luczak ED, Hall DD, Fink BD, Chen B, Yang J, Moore SA, Scholz TD, Strack S, Mohler PJ, Sivitz WI, Song LS, Anderson ME. CaMKII

determines mitochondrial stress responses in heart. Nature. 2012; 491:269–273. [PubMed: 23051746]

21. Sebag SC, Koval OM, Paschke JD, Winters CJ, Jaffer OA, Dworski R, Sutterwala FS, Anderson ME, Grumbach IM. Mitochondrial CaMKII inhibition in airway epithelium protects against allergic asthma. JCI Insight. 2017; 2
22. Joiner ML, Koval OM, Li J, He BJ, Allamargot C, Gao Z, Luczak ED, Hall DD, Fink BD, Chen B, Yang J, Moore SA, Scholz TD, Strack S, Mohler PJ, Sivitz WI, Song LS, Anderson ME. Joiner et al. reply. Nature. 2014; 513:E3.
23. Fieni F, Johnson DE, Hudmon A, Kirichok Y. Mitochondrial Ca2+ uniporter and CaMKII in heart. Nature. 2014; 513:E1–2.
24. Wirth A, Benyo Z, Lukasova M, Leutgeb B, Wettschureck N, Gorbey S, Orsy P, Horvath B, Maser-Gluth C, Greiner E, Lemmer B, Schutz G, Gutkind JS, Offermanns S. G12–G13-LARG-mediated signaling in vascular smooth muscle is required for salt-induced hypertension. Nat Med. 2008; 14:64–68. [PubMed: 18084302]
25. Ray JL, Leach R, Herbert JM, Benson M. Isolation of vascular smooth muscle cells from a single murine aorta. Methods Cell Sci. 2001; 23:185–188. [PubMed: 12486328]
26. Nguyen TT, Oh SS, Weaver D, Lewandowska A, Maxfield D, Schuler M-H, Smith NK, Macfarlane J, Saunders G, Palmer CA, Debattisti V, Koshiba T, Pulst S, Feldman EL, Hajnóczky G, Shaw JM. Loss of Miro1-directed mitochondrial movement results in a novel murine model for neuron disease. Proceedings of the National Academy of Sciences. 2014; 111:E3631–E3640.
27. Nagai T, Sawano A, Park ES, Miyawaki A. Circularly permuted green fluorescent proteins engineered to sense Ca2+ Proceedings of the National Academy of Sciences. 2001; 98:3197–3202.
28. Scott JA, Xie L, Li H, Li W, He JB, Sanders PN, Carter AB, Backs J, Anderson ME, Grumbach IM. The multifunctional Ca2+/calmodulin-dependent kinase II regulates vascular smooth muscle migration through matrix metalloproteinase 9. Am J Physiol Heart Circ Physiol. 2012; 302:H1953–1964. [PubMed: 22427508]
29. Hui DY. Intimal hyperplasia in murine models. Current drug targets. 2008; 9:251–260. [PubMed: 18336244]
30. Ginnan R, Singer HA. CaM kinase II-dependent activation of tyrosine kinases and ERK1/2 in vascular smooth muscle. Am J Physiol Cell Physiol. 2002; 282:C754–761. [PubMed: 11880263]
31. Chang BH, Mukherji S, Soderling TR. Characterization of a calmodulin kinase II inhibitor protein in brain. Proc Natl Acad Sci U S A. 1998; 95:10890–10895. [PubMed: 9724800]
32. Ginnan R, Pfleiderer PJ, Pumiglia K, Singer HA. PKC-δ and CaMKII-δ<sub>2</sub> mediate ATP-dependent activation of ERK1/2 in vascular smooth muscle. American Journal of Physiology - Cell Physiology. 2004; 286:C1281–C1289. [PubMed: 14749212]
33. Zhang J, Campbell RE, Ting AY, Tsien RY. Creating new fluorescent probes for cell biology. Nat Rev Mol Cell Biol. 2002; 3:906–918. [PubMed: 12461557]
34. Axel DI, Kunert W, Goggelmann C, Oberhoff M, Herdeg C, Kuttner A, Wild DH, Brehm BR, Riessen R, Koveker G, Karsch KR. Paclitaxel inhibits arterial smooth muscle cell proliferation and migration in vitro and in vivo using local drug delivery. Circulation. 1997; 96:636–645. [PubMed: 9244237]
35. Salu KJ, Bosmans JM, Huang Y, Hendriks M, Verhoeven M, Levels A, Cooper S, De Scheerder IK, Vrints CJ, Bult H. Effects of cytochalasin D-eluting stents on intimal hyperplasia in a porcine coronary artery model. Cardiovasc Res. 2006; 69:536–544. [PubMed: 16386237]
36. Wang X, Schwarz TL. The mechanism of Ca2+ -dependent regulation of kinesin-mediated mitochondrial motility. Cell. 2009; 136:163–174. [PubMed: 19135897]
37. De Stefani D, Raffaello A, Teardo E, Szabò I, Rizzuto R. A forty-kilodalton protein of the inner membrane is the mitochondrial calcium uniporter. Nature. 2011; 476:336–340. [PubMed: 21685888]
38. Cribbs JT, Strack S. Functional Characterization of Phosphorylation Sites in Dynamin-Related Protein 1. Methods in enzymology. 2009; 457:231–253. [PubMed: 19426871]
39. Salabei JK, Hill BG. Mitochondrial fission induced by platelet-derived growth factor regulates vascular smooth muscle cell bioenergetics and cell proliferation. Redox Biol. 2013; 1:542–551. [PubMed: 24273737]

40. Schuler MH, Lewandowska A, Di Caprio G, Skillern W, Upadhyayula S, Kirchhausen T, Shaw JM, Cunniff B. Miro1-mediated mitochondrial positioning shapes intracellular energy gradients required for cell migration. Mol Biol Cell. 2017
41. Kim DH, Wirtz D. Focal adhesion size uniquely predicts cell migration. FASEB J. 2013; 27:1351–1361. [PubMed: 23254340]
42. Mitra SK, Hanson DA, Schlaepfer DD. Focal adhesion kinase: in command and control of cell motility. Nat Rev Mol Cell Biol. 2005; 6:56–68. [PubMed: 15688067]
43. Thievessen I, Thompson PM, Berlemont S, Plevock KM, Plotnikov SV, Zemljic-Harpf A, Ross RS, Davidson MW, Danuser G, Campbell SL, Waterman CM. Vinculin–actin interaction couples actin retrograde flow to focal adhesions, but is dispensable for focal adhesion growth. The Journal of Cell Biology. 2013; 202:163–177. [PubMed: 23836933]
44. Shifman JM, Choi MH, Mihalas S, Mayo SL, Kennedy MB. Ca2+/calmodulin-dependent protein kinase II (CaMKII) is activated by calmodulin with two bound calciums. Proceedings of the National Academy of Sciences. 2006; 103:13968–13973.
45. Tsai MF, Phillips CB, Ranaghan M, Tsai CW, Wu Y, Willliams C, Miller C. Dual functions of a small regulatory subunit in the mitochondrial calcium uniporter complex. Elife. 2016; 5
46. Beutner G, Sharma VK, Giovannucci DR, Yule DI, Sheu SS. Identification of a ryanodine receptor in rat heart mitochondria. J Biol Chem. 2001; 276:21482–21488. [PubMed: 11297554]
47. Pathak D, Sepp KJ, Hollenbeck PJ. Evidence That Myosin Activity Opposes Microtubule-Based Axonal Transport of Mitochondria. The Journal of Neuroscience. 2010; 30:8984–8992. [PubMed: 20592219]
48. Bers DM. Ca2+-calmodulin-dependent protein kinase II regulation of cardiac excitation-transcription coupling. Heart Rhythm. 2011; 8:1101–1104. [PubMed: 21255680]
49. Liu Y, Sun L-Y, Singer DV, Ginnan R, Singer HA. CaMKIIδ-dependent Inhibition of cAMP-response Element-binding Protein Activity in Vascular Smooth Muscle. Journal of Biological Chemistry. 2013; 288:33519–33529. [PubMed: 24106266]
50. Mishra S, Gray CB, Miyamoto S, Bers DM, Brown JH. Location matters: clarifying the concept of nuclear and cytosolic CaMKII subtypes. Circ Res. 2011; 109:1354–1362. [PubMed: 21998325]
51. Rasmussen TP, Wu Y, Joiner M-lA, Koval OM, Wilson NR, Luczak ED, Wang Q, Chen B, Gao Z, Zhu Z, Wagner BA, Soto J, McCormick ML, Kutschke W, Weiss RM, Yu L, Boudreau RL, Abel ED, Zhan F, Spitz DR, Buettner GR, Song L-S, Zingman LV, Anderson ME. Inhibition of MCU forces extramitochondrial adaptations governing physiological and pathological stress responses in heart. Proceedings of the National Academy of Sciences. 2015; 112:9129–9134.
52. Lyle AN, Griendling KK. Modulation of Vascular Smooth Muscle Signaling by Reactive Oxygen Species. Physiology. 2006; 21:269–280. [PubMed: 16868316]
53. Poburko D, Liao CH, van Breemen C, Demaurex N. Mitochondrial regulation of sarcoplasmic reticulum Ca2+ content in vascular smooth muscle cells. Circ Res. 2009; 104:104–112. [PubMed: 19023135]
54. McCarron JG, Olson ML, Chalmers S. Mitochondrial regulation of cytosolic Ca(2)(+) signals in smooth muscle. Pflugers Arch. 2012; 464:51–62. [PubMed: 22555917]

## HIGHLIGHTS

- Mitochondrial CaMKII is present in mitoplasts of VSMC and activated by PDGF in a mechanism that is dependent upon the mitochondrial $Ca^{2+}$ uniporter.
- Inhibition of mitochondrial CaMKII or of the mitochondrial $Ca^{2+}$ uniporter decreases VSMC migration by blocking mitochondrial matrix $Ca^{2+}$ uptake.
- Inhibition of mitochondrial CaMKII prevents mitochondrial translocation to the leading edge of migrating cells, leading to decreased focal adhesion signaling and turnover.
- Selective inhibition of mitochondrial CaMKII in smooth muscle in mice reduces neointimal hyperplasia after vascular injury.

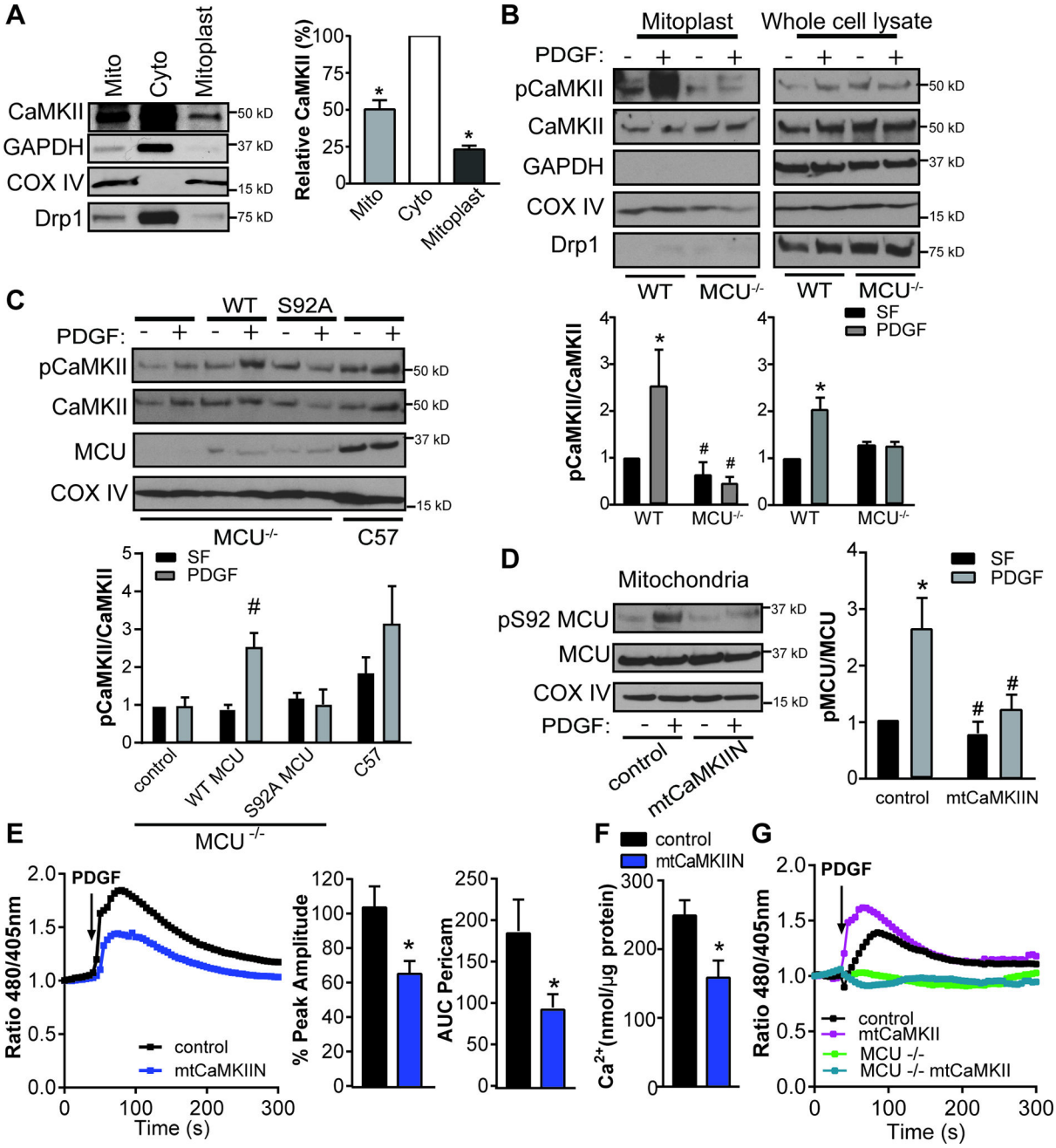


**Figure 1. Mitochondrial CaMKII regulates a feed forward circuit promoting mitochondrial Ca2+ uptake**

A) Representative immunoblot and summary data for CaMKII in mitochondrial (mito) and cytosolic (cyto) fractions and mitoplasts from VSMC. Mitoplasts (inner mitochondrial membrane and matrix) were generated by digestion of mitochondrial fractions with Proteinase K. GAPDH: cytosolic marker; Cox IV: marker of inner mitochondrial membrane; Drp1: marker of outer mitochondrial membrane. Data quantified as intensity of CaMKII to total amount of protein by BCA protein assay (n=4 independent experiments), *p<0.05 versus cytosolic fraction by Kruskall-Wallis. B) Immunoblot for active (phosphorylated, pCaMKII) and total CaMKII in whole cell lysate and mitoplast fractions of VSMC from

MCU−/− or WT mice before or after treatment with PDGF (20 ng/mL) for 15 min after serum starvation (SF). (n=5 independent experiments). C) Immunoblot for pCaMKII in mitoplast fractions of MCU−/− VSMC after transfection of WT MCUor MCU mutant Ser92 to Ala (S92A) or control and in mitoplasts of WT VSMC; treated as in (B).(n=5 independent experiments). D) Active (phosphorylated, pMCU, at S92) and total MCU inmitochondrial fractions from VSMC expressing mtCaMKIIN or control. COX IV: loading control. (n=5 independent experiments). For B-D, *p<0.05 versus control SF, #p<0.05 versus control PDGF by 2-way ANOVA. E) Representative mtPericam tracing in VSMC expressing mtCaMKIIN or control for 48 hr; arrow indicates addition of PDGF (20 ng/mL). Peak amplitude of mtPericam response normalized to peak amplitude in control cells and area under the curve (AUC) of mtPericam signal in 15 cells per condition (n=3 independent experiments). F) Ca2+ concentration by o-cresolphthalein assay in mitochondria isolated from VSMC expressing mtCaMKIIN or control for 48 hr; data were normalized to total mitochondrial protein content (n=5). G) Representative mtPericam tracing in WT or MCU −/− VSMC expressing mtCaMKII or control for 48 hr with addition of PDGF, *p<0.05 versus control by Student’s t-test.

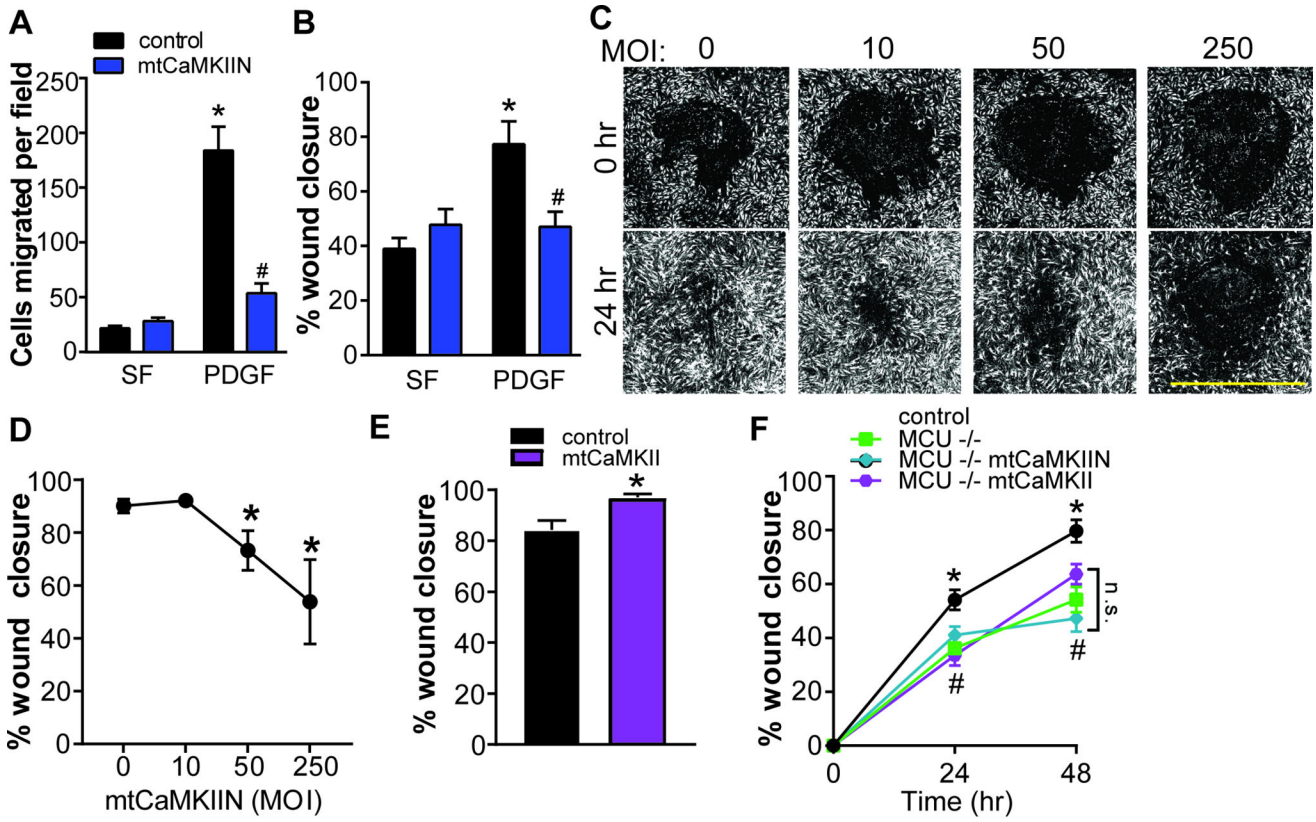


**Figure 2. Mitochondrial CaMKII inhibition blocks VSMC migration**

A) Boyden chamber migration assay in VSMC expressing mtCaMKIIN (MOI 50) or control in SF media or after treatment with PDGF (20 ng/mL) for 6 hr (n=5 independent experiments). B) Scratch wound assay in VSMC expressing mtCaMKIIN or control in SF media or after treatment with PDGF (20 ng/mL); data quantified as percent wound closure at 24 hr compared to 0 hr (n=5 independent experiments). C) Representative DPC images from high throughput scratch wound assay. WT VSMC were exposed to increasing MOIs of Ad-mtCaMKIIN; D) Migration in C quantified as percent wound closure at 24 hr compared to 0 hr; *p<0.05 versus MOI of 0 by 1-way ANOVA. E) Scratch wound assay in VSMC expressing mtCaMKII or control after treatment with PDGF; data quantified as percent wound closure at 24 hr as compared to 0 hr. *p<0.05 by Student's T-test. F) High throughput scratch wound assay in MCU−/− or WT VSMC with expression of mtCaMKIIN or mtCaMKII after treatment with PDGF. High throughput experiments were conducted in quadruplicate, with biological replicates of three independent experiments. For A, B, and F, *p<0.05 versus control in SF, #p<0.05 versus PDGF-treated control by 2-way ANOVA.

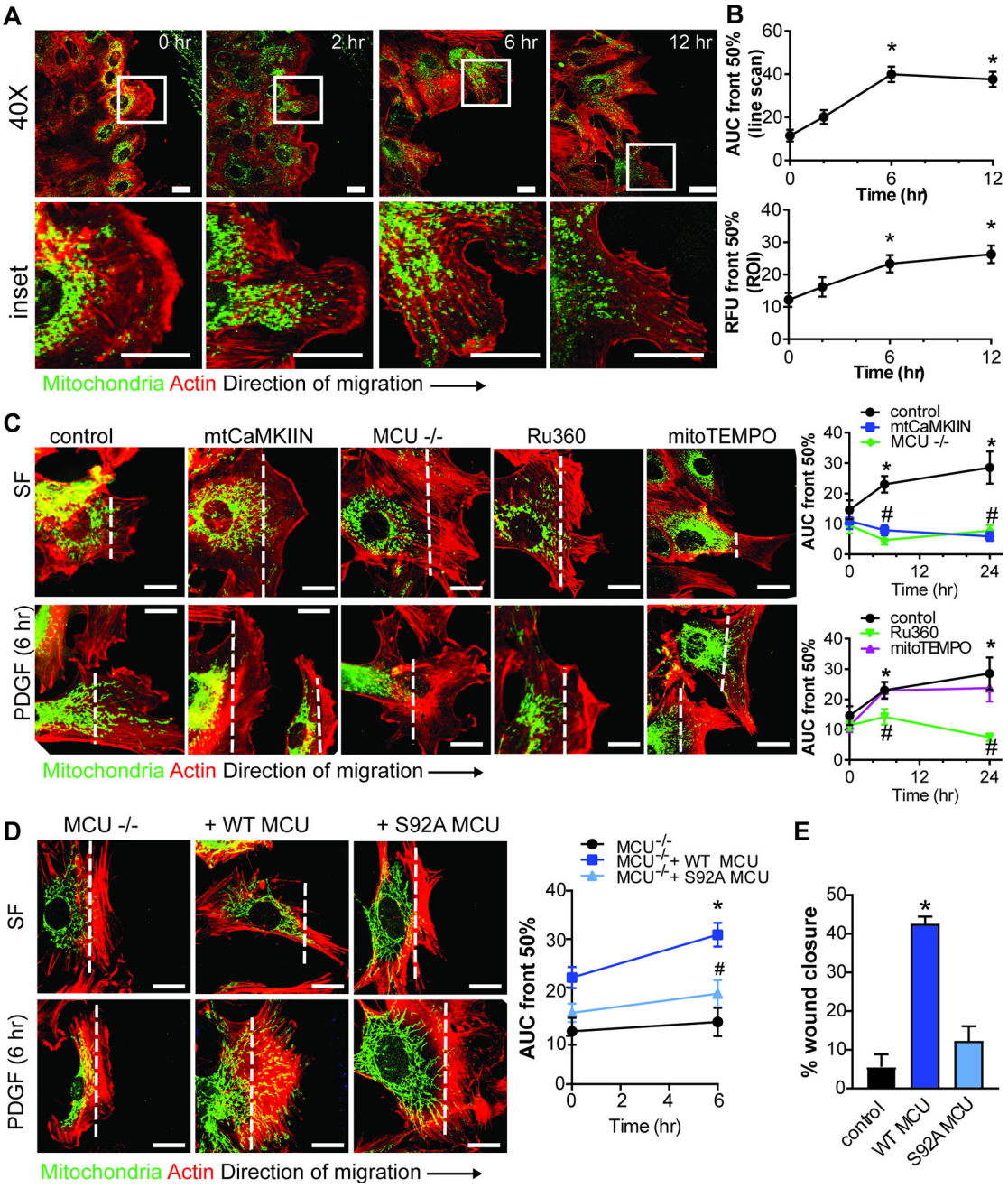


**Figure 3. Mitochondrial CaMKII inhibition blocks translocation of mitochondria to the leading edge of migrating VSMC**

A) Representative images of mitochondrial localization after scratch wound and PDGF treatment (20 ng/mL) at indicated time points; green: Ad-mtGFP; red: phalloidin-568. B) Quantification of mitochondrial distribution by line scan analysis in the leading to anterior cell areas and quantification of mitochondrial distribution expressed as percent mtGFP signal in the leading cell area (region of interest/ROI) relative to total mtGFP signal per cell (see details in methods and Supplemental Figure 5D); *p<0.05 versus control at 0 hr by 1-way ANOVA. C) Representative images of mitochondrial localization in migrating VSMC before and after PDGF treatment. Studies were performed in WT VSMC expressing

mtCaMKIIN or control, MCU−/− VSMC, or WT VSMC treated with Ru360 (1 μM) or mitoTEMPO (10 μM). mitochondrial distribution was quantified by line scan analysis. D) Representative images of mitochondrial localization in migrating MCU−/− VSMC transfected with control plasmid, WT MCU, or S92A MCU, before and after PDGF. Mitochondrial distribution was quantified by line scan analysis in the leading to anterior cell areas and expressed as percent mtGFP signal in the leading cell. Analyses were performed on 50 cells per condition (n=3 independent experiments). For C and D, *$p<0.05$ versus control at 0 hr, #$p<0.05$ versus control at the same time point by 2-way ANOVA. Scale bar= 10 μm. E) Scratch wound assay in cells from D; data quantified as percent wound closure at 6 hr after scratch as compared to 0 hr (n=3 independent experiments). *$p<0.05$ versus control by 1-way ANOVA.

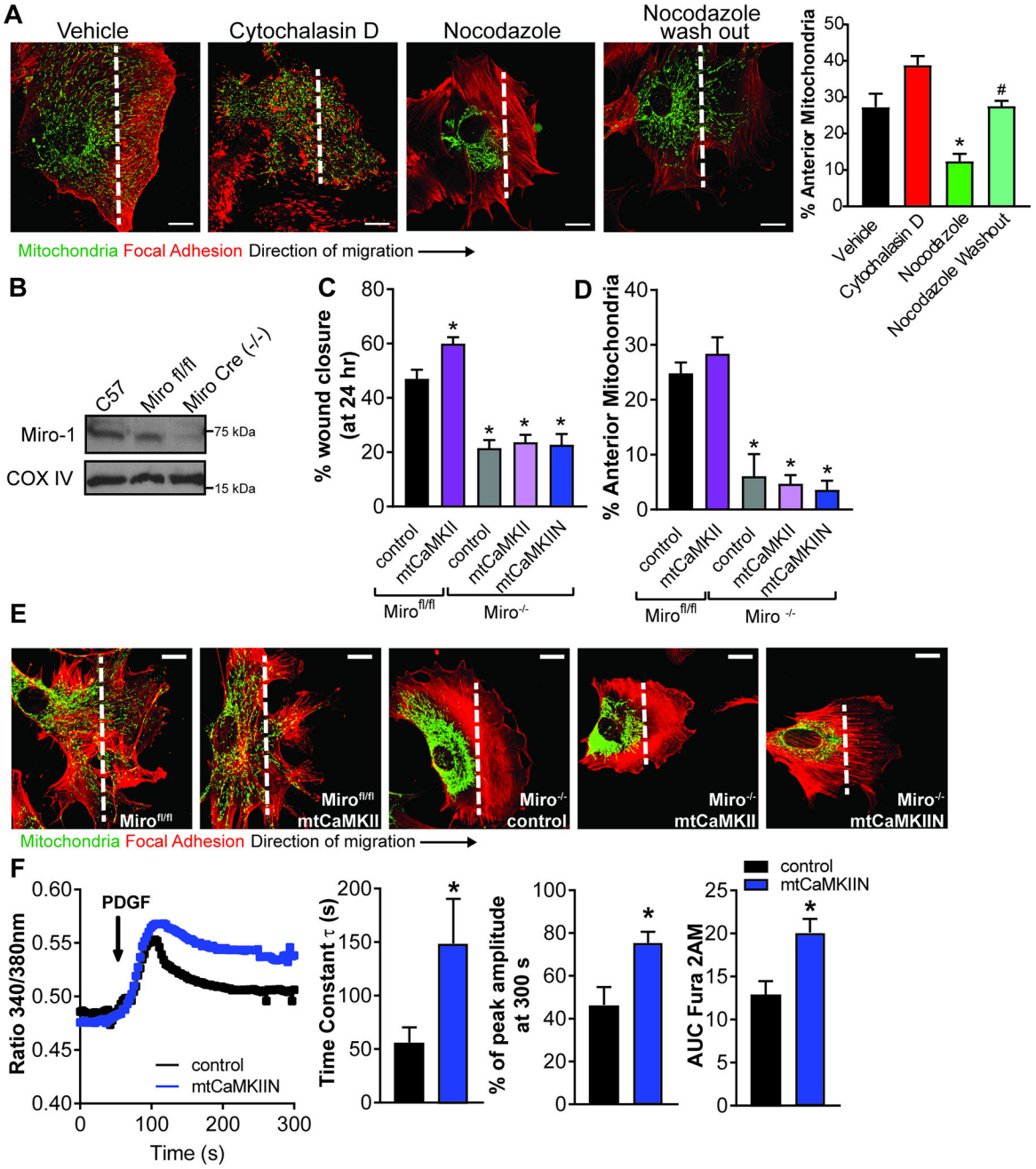


**Figure 4. mtCaMKII regulation of VSMC migration and mitochondrial mobility is dependent on the Ca2+-sensitive Miro-1**

A) Representative images of mitochondrial localization in migrating VSMC treated for 6 hr with PDGF and either actin inhibitor Cytochalasin D (0.1nM) or microtubule inhibitor Nocodazole (1 μM) or Nocodazole washed out 1 hr before fixation. Quantification of mitochondrial distribution expressed as percent mtGFP signal in the leading cell area by line scan. * $p<0.05$ vs vehicle, # $p<0.05$ vs Nocodazole by 1-way ANOVA. (20 cells over 3 independent experiments) B) Representative immunoblot of Miro-1 expression in Miro fl/fl VSMC with and without Ad5-Cre infection (MOI 10). C) VSMC migration by traditional scratch wound assay in Mirofl/fl or Cre-infected Mirofl/fl (Miro−/−) VSMC co-expressing

mtCaMKII or mtCaMKIIN. Data quantified as percent wound closure at 24 hr as compared to 0 hr, (n = 3 independent experiments). D) Quantification of mitochondrial distribution by line scan analysis in the leading to anterior cell areas expressed as percent mtGFP signal in the leading cell (30 cells over 3 independent experiments). E) Representative images of mitochondrial localization after scratch wound and PDGF treatment (20 ng/mL) at 24 hr after scratch. Green: mitochondria, AdmtGFP; red: F-actin, phalloidin-568. For A-D, *p<0.05 versus control Mirofl/fl by 1-way ANOVA. Scale bar = 10μm. F) Representative cytosolic Ca2+ tracing by Fura-2AM after 20 ng/ml PDGF (arrow) in VSMC expressing control or mtCaMKIIN. Quantification of Fura-2AM signal as time constant of decay (**τ**, left), residual signal at 300 s after PDGF relative to peak response (middle) and AUC of Fura-2AM signal (right) in 25 cells per condition in 5 independent experiments. *p<0.05 versus control by Student's T-test.

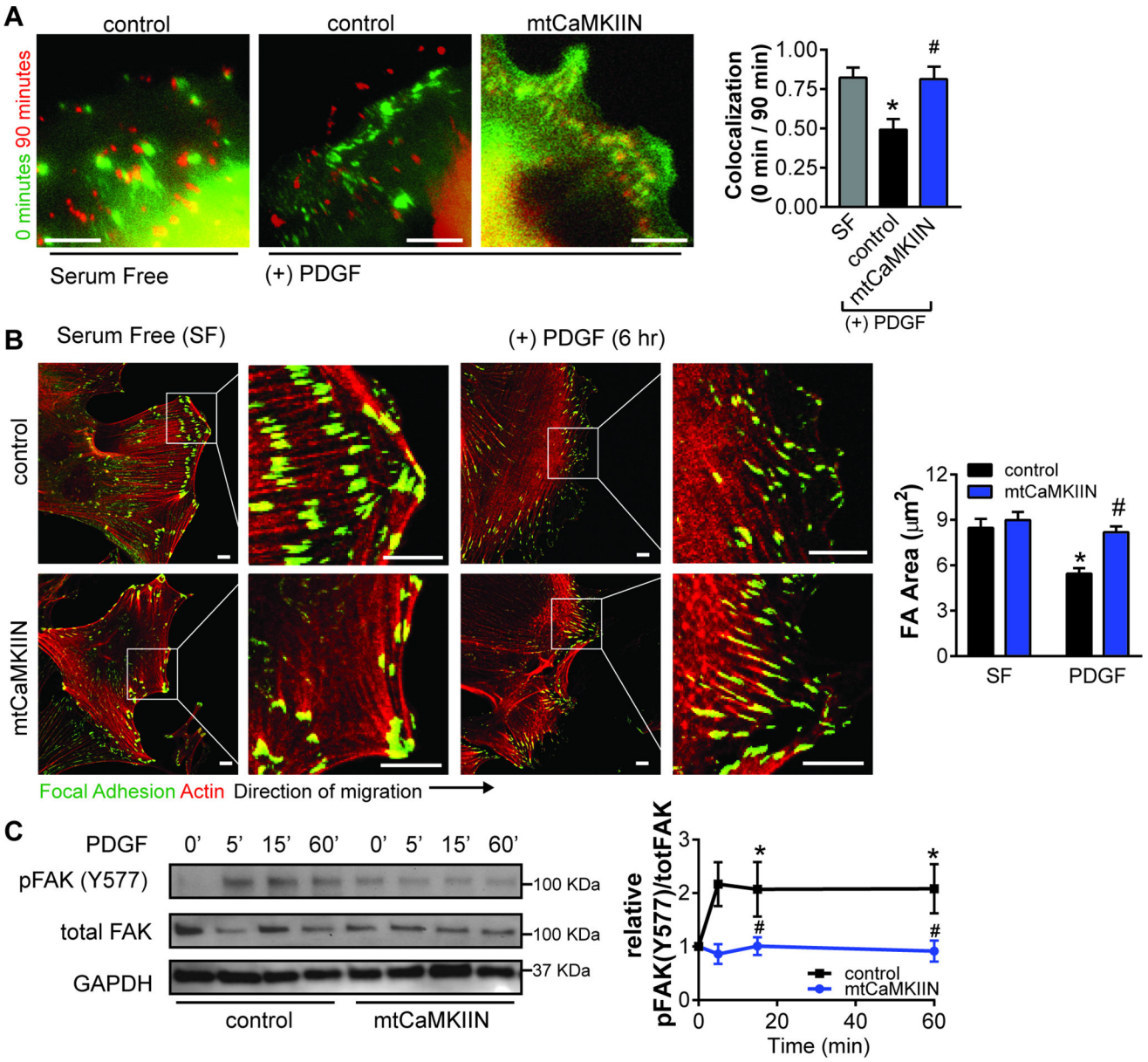


**Figure 5. Mitochondrial CaMKII inhibition alters focal adhesions dynamics**

A) Immunofluorescent overlaid time-lapse images of FA (GFP-Vinculin) at 0 (green) and 90 (red) min in VSMC expressing mtCaMKIIN or control, and in the presence of 20 ng/mL PDGF. FA colocalization at 0 and 90 min was quantified in 15 cells using CellProfiler software, *p<0.05 vs SF, #p<0.05 vs control PDGF by 1-way ANOVA. B) Representative images of focal adhesion (FA) at wound edge in VSMC expressing mtCaMKIIN or control at 0 or 6 hr after PDGF treatment in SF media with quantification of average focal adhesion size (red: phalloidin, actin;green: vinculin, FA marker). C) Immunoblots for phosphorylated (pFAK Y577) and total FAK in whole cell lysates from VSMC expressing mtCaMKIIN and treated with PDGF (20 ng/ml) for 0–60 min. Data were quantified as phosphorylated FAK (pFAK Y577) relative to total FAK, normalized to respective baseline at 0 min. GAPDH:

loading control (n=4 independent experiments). For B and C, *p<0.05 versus control SF, #p<0.05 versus control PDGF by 2-way ANOVA. Scale bar= 10 μm.

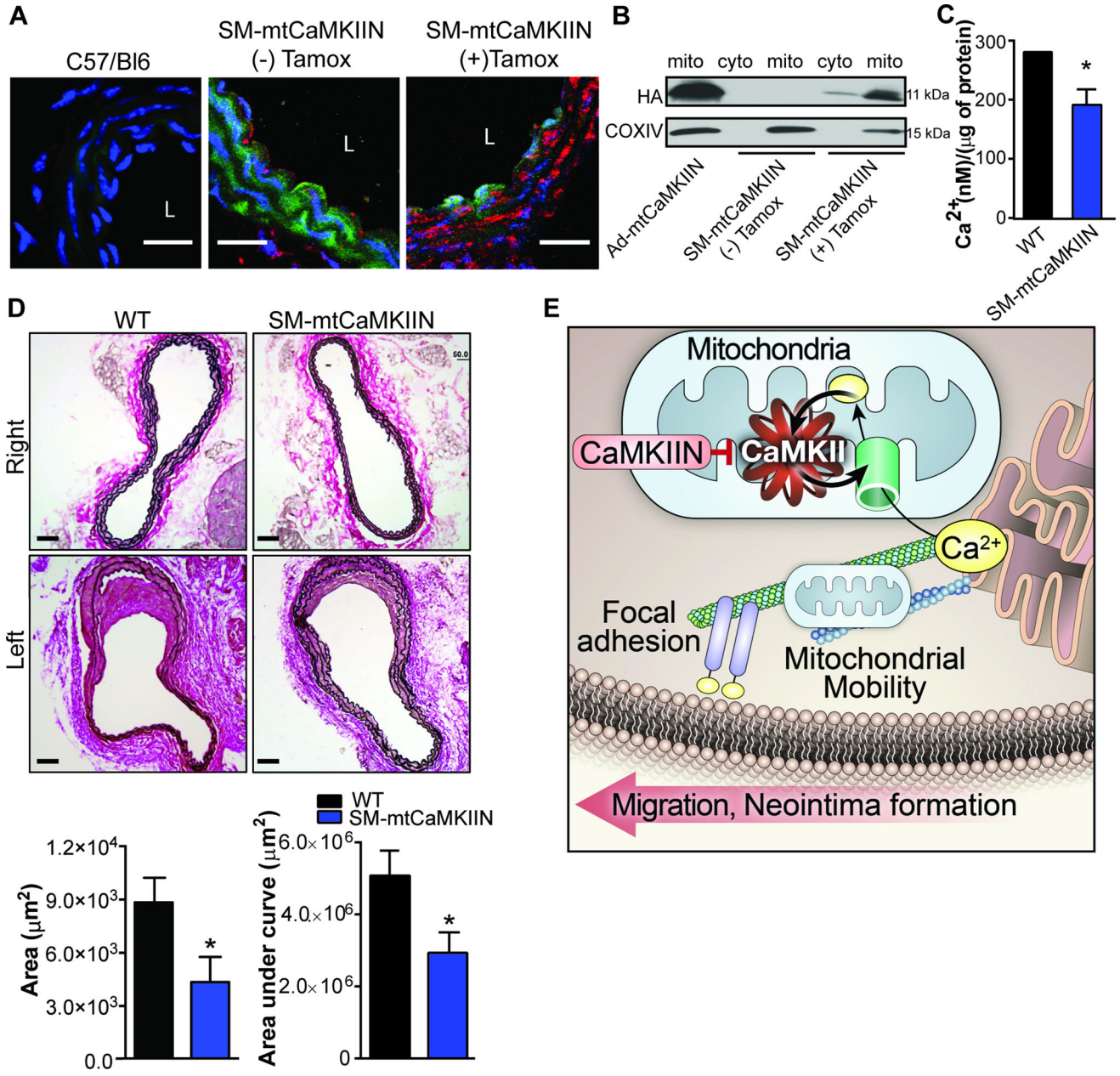


**Figure 6. Mitochondrial CaMKII inhibition in vivo blocks neointimal hyperplasia following endothelial injury**

A) Representative images of carotid arteries from C57/Bl6 (WT) and SMmtCaMKIIN mice with and without tamoxifen (Tamox) treatment, which induces cre recombination. Green: ubiquitously expressed GFP; red: mtCaMKIIN; blue: Nuclei. “L” indicates arterial lumen; scale bar= 20 μm. B) Immunoblots for hemagglutinin (HA)-tagged CaMKIIN in mitochondrial or cytosolic fractions isolated from aortas of SM-mtCaMKIIN mice with and without tamoxifen treatment. VSMC infected with Ad-mtCaMKIIN aspositive control; Cox IV: mitochondrial marker. C) $Ca^{2+}$ concentration by o-cresolphthalein assay in mitochondria isolated from aortas of SM-mtCaMKIIN or WT littermate controls (SM-Cre mice). Data were normalized to total mitochondrial protein measured by BCA assay (n=5 mice per

genotype). D) Representative images of Verhoeff's Van Gieson staining of left common carotid arteries at 28 days after endothelial injury in WT or SM-mtCaMKIIN mice. Contralateral (right) common carotid artery serves as uninjured control with quantification of neointimal area at 200 μm from the carotid bifurcation and neointimal volume calculated from all neointimal areas within 500 μm from carotid bifurcation; scale bar= 50 μm, n=12 mice per genotype. *$p<0.05$ versus WT by Student's T-test. E) Graphic representation of the proposed pathway by which mitochondrial CaMKII regulation of mitochondrial $Ca^{2+}$, mobility, and VSMC migration. mtCaMKII regulates a feed-forward circuit that promotes mitochondrial $Ca^{2+}$ uptake. Inhibition of mtCaMKII leads to decreased mitochondrial $Ca^{2+}$ uptake, leading to decreased $Ca^{2+}$ clearance in the cytosol and mitochondrial arrest. This prevents mitochondria from translocating to focal adhesions, thus inhibiting VSMC migration and neointima formation.